HHS Public Access

Author manuscript

*Adv Healthc Mater*. Author manuscript; available in PMC 2015 October 13.

Published in final edited form as:

*Adv Healthc Mater*. 2013 July ; 2(7): 945–951. doi:10.1002/adhm.201200430.

# Exposure to Carbon Nanotubes Leads to Changes in the Cellular Biomechanics

**Chenbo Dong**

Department of Chemical Engineering, West Virginia University, Morgantown WV, 26506, USA

**Dr. Michael L. Kashon**

Toxicology and Molecular Biology Branch, National Institute for Occupational Safety and Health, Morgantown WV, 26505, USA

**David Lowry**

Toxicology and Molecular Biology Branch, National Institute for Occupational Safety and Health, Morgantown WV, 26505, USA

**Prof. Jonathan S. Dordick**

Department of Chemical and Biological Engineering, Rensselaer Polytechnic Institute, Troy, NY, 12180, USA

**Dr. Steven H. Reynolds**

Toxicology and Molecular Biology Branch, National Institute for Occupational Safety and Health, Morgantown WV, 26505, USA

**Prof. Yon Rojanasakul**

Department of Basic Pharmaceutical Sciences, West Virginia University, Morgantown WV, 26506, USA

**Dr. Linda M. Sargent***

Toxicology and Molecular Biology Branch, National Institute for Occupational Safety and Health, Morgantown WV, 26505, USA

**Prof. Cerasela Zoica Dinu***

Department of Chemical Engineering, West Virginia University, Morgantown WV, 26506, USA

Carbon nanotubes (CNTs) are rolled-up cylindrical structures of single (single-walled carbon nanotube-SWCNT) or multiple (multi-walled carbon nanotube-MWCNT) sheets of graphene that have high aspect ratio,[1] high electrical and thermal conductivity,[2] ultra-light weight,[3] and high mechanical strength.[4] Their unique properties provide a tremendous potential for applications in fields as diverse as electronics,[5] aerospace industries,[6] sensors,[7] actuators,[8] or composites.[9] Based on their properties, researchers have also been exploring CNTs potential for biological and biomedical applications as drug delivery systems,[10] substrate for cells growth in tissue regeneration,[11] therapeutic

cerasela-zoica.dinu@mail.wvu.edu. lqs1@cdc.gov.

**Supporting Information**

Supporting Information is available from the Wiley Online Library or from the author.

agents,[11] or as vectors for gene transfection.[12] Such broad applications of CNTs have led to an increased production level and thus increased concerns regarding human and environmental exposure. Further, given their applications in the biomedical field,[13,14] understanding how biological systems interact with this nanomaterial is urgently needed to create safer therapies,[14,15] and to regulate occupational exposures.[16,17]

Recent work has shown that *in vitro* and *in vivo* exposure to SWCNTs can lead to alterations in DNA structure.[18,19] For instance, our recent studies have shown that 24 to 72 h exposure of epithelial cells to SWCNTs induced centrosome fragmentation and aneuploidy[18,20] similar to the genotoxin vanadium pentoxide.[21] Likewise, cellular exposure to MWCNT disrupted the mitotic spindle by association with microtubules,[22] induced polyploidy[17] and changes in chromosome number in a fashion similar to crocidolite asbestos.[20,23,24] CNTs genotoxicity has been attributed to a variety of factors including metal impurities, length, size, number of walls, surface area, dispersion, and/or CNTs surface functionalization.[23,25] Furthermore, genotoxicity associated with CNTs-cellular exposure has been shown to lead to potential carcinogenic risks similar to ones found for asbestos.[26]

Studies have shown that cancer development is related to alterations in cell mechanical phenotype including changes in the cell structure,[27] morphology,[28] and responses to mechanical stimuli.[29] The mechanical phenotype of cells is regulated by dynamic networks of cytoskeletal filaments (i.e., cellular scaffold) such as microtubule and actin,[30] and by signaling molecules.[31] Alterations of mechanical phenotype of individual cells could reveal important information about changes in cytoskeletal networks, with changes in the cell rigidity being correlated with malignant transformation and cancer progression.[32] Studies have shown that SWCNTs can induce actin bundling and influence cell proliferation in exposed cells.[33] Other studies have shown that MWCNTs interact with microtubules, blocking mitosis and leading to cell death by apoptosis.[22] Given the complex effects of CNTs on increased genetic instability with potential carcinogenic risks, as well as the association of CNTs with the cytoskeletal filaments, it is important that we begin to understand how exposure to these nanomaterials affects cellular biomechanics that may be functionally linked to mechanisms involved in CNTs-induced genotoxicity and potentially in cancer development.

Studies have demonstrated the effectiveness of nanoindentation based on atomic force microscopy (AFM) on assessing differences between cancer cells and normal cells based on their mechanics. For instance, displacement curves of the AFM cantilever versus vertical position of the scanner demonstrated that cancer cells have greater variability in their force behavior when compared to normal cells.[29,34] Also, nanomechanical-based functional analysis has been used to detect metastatic tumor cells in bodily fluids, with changes in nanomechanical properties of such cells being associated with shape changes inherent to metastatic adenocarcinoma cells.[32,35] Herein, we have examined the biomechanics of epithelial cells exposed to MWCNTs with diameters of 10–20 nm and lengths <1 μm. Our hypothesis was that MWCNTs permissible exposure limit[36] leads to morphological and cytomechanical cellular changes that can be detected using nanoindentation.[32] Our observations suggest that measures of the mechanical properties of cells upon MWCNTs exposure could be used as indicators of their biological state with MWCNTs-induced

increased cellular stiffness suggesting the potential for genetic instability and cancer development.

We used acid-washed MWCNTs prepared from pristine MWCNTs incubated in a mixture of sulfuric and nitric acids for 1 h followed by subsequent washing steps in water.[37] **Figures 1**a and 1b depict the Raman spectra of pristine and 1 h acids-washed MWCNTs. Both samples showed a small D band (disorder mode) at ~1340 $cm^{-1}$; the D band was wider and had a higher frequency for the 1 h acids-washed sample. This shift indicates that acids treatment introduced additional functional groups, i.e., free carboxylic acids groups.[38] The 1 h acids-washed MWCNTs spectra also showed a shift in the G mode (1585 nm) with increased intensity towards higher frequency, an indication of metal catalyst removal, increase in the number of functional groups having electron-accepting capability, and/or increase in amorphous carbon (see Supporting Information Table S1). The ratio of relative intensity of D to G peaks ($I_D/I_G$) is defined as the degree of functionalization;[39] the higher this ratio, the higher the level of functionalization. Our results indicate that $I_D/I_G$ was 0.45 for pristine and 0.78 for 1 h acids-washed MWCNTs, further confirming that acids treatment greatly increased the number of functional groups on the nanotubes.

The presence of the carboxyl groups was further confirmed by energy-dispersive X-ray spectroscopy. Acids washing led to removal of catalysts and impurities (i.e., 25% decrease in Fe in the 1h acids-washed sample when compared with the pristine sample) and an increase of 17% in the O content. As a result of free carboxylic acid groups being added upon treatment,[38] the 1 h acids-washed MWCNTs have a higher dispersity (see Supporting Information Table S2) when compared to pristine MWCNTs. Further, their lengths were reduced as confirmed by atomic force microscopy (AFM) (final length 947 ± 451 nm/mean ± standard deviation; see Supporting Information Table S3).

Cell culture experiments were performed using a complete randomized block design. Briefly, human bronchial epithelial cells (BEAS-2B) seeded at the concentration of $10^5$ cells were exposed to 24 μg/$cm^2$ 1 h acids-washed MWCNTs (a permissible exposure limit for particulates not otherwise regulated[36]) fully dispersed in culture media, for 24 h at 37 °C. Upon exposure, “free” 1 h acids-washed MWCNTs (i.e., 1 h acids-washed MWCNTs not associated with or taken up by the cells) were removed by several washing steps.

Contact mode AFM was used to probe the topography and biomechanics of the cells.[40] To avoid changes in cellular properties during observation and analysis, samples were fixed with 4% glutaraldehyde. Fixed cell topography was imaged by establishing mechanical contact between the AFM tip and individual cells in nonzero imaging force[40] with a scan rate of 0.25 Hz and a pixel resolution of 176 nm/pixel (**Figure 2**a). A representative control cell body (i.e., for a cell not exposed to 1 h acids-washed MWCNTs) is shown in Figure 2b while a representative cell exposed to 1 h acids-washed MWCNTs is shown in Figure 2c. The surface of the control cell appeared smooth and homogenous, in contrast with a significantly different morphology and increased roughness observed for the cell exposed to 1 h acids-washed MWCNTs. Interestingly, the exposed cells also showed a significant increase in their average surface area (~37.7%, $p < 0.05$) when compared with control cells.

However, the increase in average height (~10.5%) observed for the exposed cells was not significant when compared to control cells (Figure 2d).

We studied cell biomechanics in response to exposure to 1 h acids-washed MWCNTs. Control cells (**Figure 3**a) were elastically mapped using the extended Hertz model and considering an infinitely stiff indenter with a selected geometry of the AFM tip (i.e. conical) and a flat, deformable substrate.[41,42] The resulting indentation image of a control cell (Figure 3b) shows Young's modulus of the cell body in the 100–250 kPa range (Figure 3c); the higher stiffness noted at the cell periphery (up to 600 kPa) may be due to the underlying substrate.[40] The highest region of the cell (dashed red in Figure 3a; the rest of the cell body is dashed black) corresponds to the cell nucleus; this region appears softer when compared to the rest of the cell and has Young's modulus values in between 40–80 kPa (Figure 3d).

**Table 1** shows the Young's modulus distribution of control cells and cells exposed to 1 h acids-washed MWCNTs for 24 h. The cells exposed to 1 h acids-washed MWCNTs showed a significant increase in the Young's modulus when compared with control cells ($p < 0.05$). Specifically, the exposed cells have significant difference in their stiffness when compared to control cells, with an overall increase of 29.8% in their Young's modulus and an increase of 36.6% in their cell nucleus Young's modulus. Further, for the cells incubated with 1 h acids-washed MWCNTs there was a considerable shift of the Young's modulus towards higher values at the cell nucleus. For instance, in between 100–400 kPa there is an increase from 35.90% to 58.17% from control to 1 h acids-washed MWCNTs exposed cells. Even more, the nucleus of the cells exposed to MWCNTs reached values as high as 600 kPa. The Gaussian fits of the cells exposed to 1 h acids-washed MWCNTs for the perinuclear or nuclear regions are shown in Figure 3e and 3f respectively, while the average Young's modulus of the exposed cells when compared to control cells is shown in Figure 3g. In control, when cells were incubated with 1 h acids-washed MWCNTs only for 1 h there was no shift in the Young's modulus of the exposed cells when compared to control cells (see Supporting Information Table S4). Even further, there was no significantly relevant shift observed neither for the perinuclear nor for the nuclear regions when the Gaussian fits of the cells exposed to 1 h acids-washed MWCNTs for 1 h was compared to the Gaussian fits of control cells (see Supporting Information Figure S1). It was however noted that the stiffness for both control and 1 h acids-washed MWCNT-exposed cells was about one order of magnitude larger than for living cells.[43] This could be the result of either: (1) cell fixation with glutaraldehyde;[40] (2) large stiffness of the substrate;[40] or (3) the induced strains in the cells caused by the tip indented at low speed (i.e., 0.25 kHz).[44]

Our findings are significant in that they relate for the first time the cellular changes in biomechanics upon MWCNTs exposure with the potential for genotoxicity and cancer development in the MWCNTs-exposed cells. Specifically, our study shows that after 24 h exposure, MWCNTs localize at the cell nucleus, with nanotube localization inducing changes in the nucleus mechanics by increasing its stiffness and overall Young's modulus with more than 36.6% than for control cells (either cells exposed to 1 h acids-washed MWCNTs for 1 h or to the control cells). Combining our data with previous reports that indicate that MWCNTs interact with microtubules,[22,46] the mitotic spindle,[22] DNA and cell division apparatus,[17,18] we propose now that the observed stiffness due to exposure to

1 h acids-washed MWCNTs could lead the reorganization of the three-dimensional cellular cytoskeletal network. Such reorganization could potentially disrupt the mitotic spindle,[22] inducing errors in chromosome numbers to be propagated through further cellular division[19] as characteristics of cancer cells.[48] This is also in agreement with comparative gene expression analysis that indicated that the molecular basis of the cell stiffness is reflective of the extensive molecular changes in cytoskeleton remodeling pathways[45] and with previous reports that have shown that tumorgenic and metastatic potential are linked to cellular deformability.[47]

The demonstrations performed in this study are the first quantitative biomechanical measurements on how nanoindentation can be used as a valuable tool to obtain quantitative maps and spatial patterns of local cellular biomechanical changes upon exposure of human lung epithelial cells to MWCNTs. Our findings suggest significant differences in the distribution of elastic properties between the lung epithelial cells incubated with MWCNTs and control cells, with the nanomaterial incubation leading to stiffer and wider modulus distributions and reflecting nuclei moduli significantly stiffer than the cytoplasmic ones. The observations described herein may also suggest a new approach to the consideration of deleterious effects associated with CNTs exposure, and their characterization by means of forces and mechanical parameters. Our findings also provide complex data for modeling the processes associated with mechanotransduction and could lead to improved understanding of the changes in the physiological pulmonary function upon CNTs exposure and how this exposure is associated with CNT-induced genetic instability.

## Experimental Section

### Multi-walled carbon nanotubes (MWCNTs) acid washing

Commercial multi-walled carbon nanotubes (MWCNTs, Nanolab Inc. PD15L5-20, USA) were suspended in a mixture of 3:1 (V/V) concentrated sulfuric (96.4%, Fisher, USA) and nitric (69.5%, Fisher, USA) acids and placed for 1 h in a water and ice bath sonicator (Branson 2510, Fisher, USA). Subsequently the mixture was diluted in deionized (di) water and filtered through a GTTP 0.2 μm polycarbonate filter membrane (Fisher, USA); the filtration process was repeated at least 6 times to remove catalysts or impurities.

### Characterization of MWCNTs

Energy dispersive X-ray analysis (EDX) allowed quantitative elemental analysis of pristine and 1 h acids-washed MWCNTs. Samples (1 mg/ml in water) were vacuum dried on silica wafers. Experiments were performed on a Hitachi S-4700 Field Emission Scanning Electron Microscope (USA) combining secondary (SE) and backscattered (BSE) electron detection in a single unit and operating at 20 kV.

The chemical structure of MWCNTs (both pristine and 1 h acids-washed) was investigated using Raman spectroscopy. Experiments were performed at room temperature using a Renishaw InVia Raman Spectrometer (CL532-100, 100 mW, USA). Nanotubes (1 mg) were mounted on clean glass slides (Fisher, USA) and irradiated through a 20× microscope objective using an argon ion ($Ar^+$) laser beam with a spot size of <0.01 $mm^2$ operating at

514.5 nm. Low laser energy of <0.5 mV and an exposure time of 10 sec prevented local heating effects; scans in 100 to 3200 $cm^{-1}$ range were acquired.

An atomic force microscope (AFM) and Si tips (AC240TS, 50 to 90 kHz, Asylum Research, USA) were used to investigate the length of both pristine and 1 h acids-washed MWCNTs. Nanotubes (10 μg/mL, pristine or 1 h acids-washed) were deposited on mica surfaces (9.5 mm diameter, 0.15–0.21 mm thickness, Electron Microscopy Sciences, USA) and dried under vacuum. Scans of 10 μm × 10 μm area were acquired using tapping mode in air; at least 30 individual nanotubes from different slides were analyzed for an average length distribution.

### MWCNTs solubility tests

The solubility of pristine and 1 h acids-washed MWCNTs in water, phosphate buffer or Dulbecco modified Eagle with or without fetal bovine serum were determined by centrifuging the corresponding solution suspension (initial concentration 3 mg $mL^{-1}$ for pristine and 1 h acids-washed MWCNTs) at 3000 rpm for 5 min and then filtering the supernatant (0.8 mL) through a 0.2-μm GTTP membrane. After complete drying under vacuum, the amount of pristine and 1 h acids-washed MWCNTs on the membrane was weighted and the solubility was calculated based on the initial amount and volume of the starting sample.

### Cell culture and cell treatment

Immortalized human bronchial epithelial cells (BEAS-2B, ATCC, USA) of passages 4-6 were cultured in DMEM media (Invitrogen, USA) supplemented with 10% fetal bovine serum (Invitrogen, USA). Cells of at least 90% purity and 80% viability from a single lot were used for all experiments.

BEAS-2B cells plated in 50 mm parallel culture dishes (BD Biosciences, USA) at a density of $1 \times 10^5$ cells per dish for 24 h or 1 h were exposed to 24 $\mu g/cm^2$ MWCNTs. For biomechanical analysis, the BEAS-2B cells (control-unexposed or exposed) were washed with phosphate saline buffer (PBS, Invitrogen, USA) two times for 5 min each and then fixed with 4% glutaraldehyde solution (Sigma, USA) for 30 min, washed again and further analyzed in PBS.

### Biomechanical studies

A commercially available atomic force microscope (AFM) integrated with an inverted fluorescence microscope (MFP-3D-BIO; Asylum Research, TE2000-U, USA) was used to probe the cellular topography and mechanical properties of the cellular samples. Cells were imaged in liquid Petri dishes using contact mode and Olympus TR400-PB cantilevers with spring constants of 0.09 N/m. Scan speeds at 0.25 Hz, pixel resolutions of 512, and scan angle of $90^o$ (with respect to the cantilever) were employed for the topography imaging. Cellular biomechanics was investigated using the Sneddon's modification of the Hertz model developed for a four-sided pyramid.[41,42] Specifically, force–displacement curves were converted into force-indentation curves[49] with the assumption that the indented

sample is extremely thick in comparison to the indentation depth. The cell stiffness (Young's modulus, *E*) was related to the indentation of the tip, δ through equation (1):

$$E=\frac{\pi}{2}\frac{\rceil - v^2 F}{tan\alpha\delta^2},$$

where the Poisson's ratio for the cells was $v = 0.5$[42] and α = 36° is the open angle of the tip. The loading force on the cantilever *F* was calculated by simultaneously recording cantilever's deflection multiplied by the spring constant of the cantilever ($k = 0.09$ N/m).

### Statistical analysis

The cell culture experiments were performed using a randomized complete block design. Each block contained 2 cell culture dishes that were randomly assigned either vehicle or MWCNTs treatment. Three blocks were run in total. For each culture, 4 to 7 cells were examined and averaged into a single value as cells from the same culture are not independent. The variables, including Young's modulus, surface area and height were analyzed using the Proc Mixed procedure in SAS/Stat for Windows (SAS, Cary NC) with experimental block modeled as a random effect. All differences were considered statistically significant at $p < 0.05$.

## Supplementary Material

Refer to Web version on PubMed Central for supplementary material.

## Acknowledgements

C. D. acknowledges financial support from the NanoSAFE. L. M. S. acknowledges support from NORA 927000Y. C. Z. D. acknowledges support from the NanoSAFE and National Science Foundation (NSF) grant EPS-1003907. Authors acknowledge use of the WVU Shared Research Facilities.

## References

[1]. a) Higginbotham AL, Kosynkin DV, Sinitskii A, Sun ZZ, Tour JM. ACS Nano. 2010; 4:2059. [PubMed: 20201538] b) Yu WJ, Hou PX, Zhang LL, Li F, Liu C, Cheng HM. Chem. Commun. 2010; 46:8576.

[2]. a) Byrne MT, Gun'ko YK. Adv. Mater. 2010; 22:1672. [PubMed: 20496401] b) Meng CZ, Liu CH, Fan SS. Adv. Mater. 2010; 22:535. [PubMed: 20217749]

[3]. Saeed K. J. Chem. Soc. Pakistan. 2010; 32:559.

[4]. Liu K, Sun YH, Lin XY, Zhou RF, Wang JP, Fan SS, Jiang KL. Acs Nano. 2010; 4:5827. [PubMed: 20831235]

[5]. Chen PC, Shen GZ, Shi Y, Chen HT, Zhou CW. Acs Nano. 2010; 4:4403. [PubMed: 20731426]

[6]. Nouni N, Ziaei-Rad S, Adibi S, Karimzadeh F. Mater. Design. 2012; 34:1.

[7]. Xu XA, Jiang SJ, Hu Z, Liu SQ. Acs Nano. 2010; 4:4292. [PubMed: 20565121]

[8]. Chun KY, Oh Y, Rho J, Ahn JH, Kim YJ, Choi HR, Baik S. Nat. Nanotechnol. 2010; 5:853. [PubMed: 21113161]

[9]. Lota G, Fic K, Frackowiak E. Energ. Environ. Sci. 2011; 4:1592.

[10]. Li RB, Wu R, Zhao L, Wu MH, Yang L, Zou HF. Acs Nano. 2010; 4:1399. [PubMed: 20148593]

[11]. Namgung S, Baik KY, Park J, Hong S. Acs Nano. 2011; 5:7383. [PubMed: 21819114]

[12]. Nunes A, Amsharov N, Guo C, Van den Bossche J, Santhosh P, Karachalios TK, Nitodas SF, Burghard M, Kostarelos K, Al-Jamal KT. Small. 2010; 6:2281. [PubMed: 20878655]

[13]. a) Chen JY, Chen SY, Zhao XR, Kuznetsova LV, Wong SS, Ojima I. J. Am. Chem. Soc. 2008; 130:16778. [PubMed: 19554734] b) Singh MK, Shokuhfar T, Gracio JJD, de Sousa ACM, Fereira JMD, Garmestani H, Ahzi S. Adv. Funct. Mater. 2008; 18:694.c) Liu Z, Chen K, Davis C, Sherlock S, Cao QZ, Chen XY, Dai HJ. Cancer Res. 2008; 68:6652. [PubMed: 18701489] d) Choi JH, Nguyen FT, Barone PW, Heller DA, Moll AE, Patel D, Boppart SA, Strano MS. Nano Lett. 2007; 7:861. [PubMed: 17335265]

[14]. Kang B, Yu DC, Dai YD, Chang SQ, Chen D, Ding YT. Small. 2009; 5:1292. [PubMed: 19274646]

[15]. a) Dothager RS, Piwnica-Worms D. Cancer Res. 2011; 71:5611. [PubMed: 21862634] b) Liu Z, Fan AC, Rakhra K, Sherlock S, Goodwin A, Chen XY, Yang QW, Felsher DW, Dai HJ. A ngew Chem. Int. Edit. 2009; 48:7668.c) Bhirde AA, Patel V, Gavard J, Zhang GF, Sousa AA, Masedunskas A, Leapman RD, Weigert R, Gutkind JS, Rusling JF. ACS Nano. 2009; 3:307. [PubMed: 19236065]

[16]. a) Han JH, Lee EJ, Lee JH, So KP, Lee YH, Bae GN, Lee SB, Ji JH, Cho MH, Yu IJ. Inhal. Toxicol. 2008; 20:741. [PubMed: 18569096] b) Ryman-Rasmussen JP, Tewksbury EW, Moss OR, Cesta MF, Wong BA, Bonner JC. Am. J. Resp. Cell. Mol. 2009; 40:349.

[17]. Sargent LM, Reynolds SH, Castranova V. Nanotoxicology. 2010; 4:396. [PubMed: 20925447]

[18]. Sargent LM, Hubbs AF, Young SH, Kashon ML, Dinu CZ, Salisbury JL, Benkovic SA, Lowry DT, Murray AR, Kisin ER, Siegrist KJ, Battelli L, Mastovich J, Sturgeon JL, Bunker KL, Shvedova AA, Reynolds SH. Mutat. Res. Genet. Toxicol. Environ. Mutagen. 2012; 745:28.

[19]. Hubbs AF, Mercer RR, Benkovic SA, Harkema J, Sriram K, Schwegler-Berry D, Goravanahally MP, Nurkiewicz TR, Castranova V, Sargent LM. Toxicol. Pathol. 2011; 39:301. [PubMed: 21422259]

[20]. Muller J, Decordier I, Hoet PH, Lombaert N, Thomassen L, Huaux F, Lison D, Kirsch-Volders M. Carcinogenesis. 2008; 29:427. [PubMed: 18174261]

[21]. Ma S, Trivinos-Lagos L, Graf R, Chisholm RL. J. Cell. Biol. 1999; 147:1261. [PubMed: 10601339]

[22]. Rodriguez-Fernandez L, Valiente R, Gonzalez J, Villegas JC, Fanarraga ML. Acs Nano. 2012; 6:6614. [PubMed: 22769231]

[23]. Asakura M, Sasaki T, Sugiyama T, Takaya M, Koda S, Nagano K, Arito H, Fukushima S. J. Occup. Health. 2010; 52:9.

[24]. Patlolla AK, Hussain SM, Schlager JJ, Patlolla S, Tchounwou PB. Environ. Toxicol. 2010; 25:608. [PubMed: 20549644]

[25]. a) Sargent LM, Shvedova AA, Hubbs AF, Salisbury JL, Benkovic SA, Kashon ML, Lowry DT, Murray AR, Kisin ER, Friend S, McKinstry KT, Battelli L, Reynolds SH. Environ. Mol. Mutagen. 2009; 50:708. [PubMed: 19774611] b) Barillet S, Simon-Deckers A, Herlin-Boime N, Mayne-L'Hermite M, Reynaud C, Cassio D, Gouget B, Carriere M. J. Nanopart. Res. 2010; 12:61.c) Mouchet F, Landois P, Sarremejean E, Bernard G, Puech P, Pinelli E, Flahaut E, Gauthier L. Aquat. Toxicol. 2008; 87:127. [PubMed: 18313771]

[26]. Nagai H, Okazaki Y, Chew SH, Misawa N, Yamashita Y, Akatsuka S, Ishihara T, Yamashita K, Yoshikawa Y, Yasui H, Jiang L, Ohara H, Takahashi T, Ichihara G, Kostarelos K, Miyata Y, Shinohara H, Toyokuni S. Proc. Natl. Acad. Sci. U. S. A. 2011; 108:E1330. [PubMed: 22084097]

[27]. Fearon ER. Annu. Rev. Pathol.-Mech. 2011; 6:479.

[28]. Yee DS, Tang YX, Li XS, Liu ZB, Guo Y, Ghaffar S, McQueen P, Atreya D, Xie J, Simoneau AR, Hoang BH, Zi XL. Mol. Cancer. 2010; 9

[29]. Iyer S, Gaikwad RM, Subba-Rao V, Woodworth CD, Sokolov I. Nat. Nanotechnol. 2009; 4:389. [PubMed: 19498402]

[30]. Hawkins T, Mirigian M, Yasar MS, Ross JL. J. Biomech. 2010; 43:23. [PubMed: 19815217]

[31]. Xu Y, Zhu XW, Hahm HS, Wei WG, Hao EG, Hayek A, Ding S. Proc. Natl. Acad. Sci. U. S. A. 2010; 107:8129. [PubMed: 20406903]

[32]. Cross SE, Jin YS, Rao J, Gimzewski JK. Nat. Nanotechnol. 2007; 2:780. [PubMed: 18654431]

[33]. Holt BD, Short PA, Rape AD, Wang YL, Islam MF, Dahl KN. ACS Nano. 2010; 4:4872. [PubMed: 20669976]

[34]. Plodinec M, Loparic M, Monnier CA, Obermann EC, Zanetti-Dallenbach R, Oertlem P, Hyotylam JT, Aebi U, Bentires-Alj M, Lim RYH, Schoeneberger C. Nat. Nanotechnol. 2012; 7:757. [PubMed: 23085644]

[35]. Gavara N, Chadwick RS. Nat. Nanotechnol. 2012; 7:733. [PubMed: 23023646]

[36]. Hubbs A, Greskevitch M, Kuempel E, Suarez F, Toraason M. J. Toxicol. Env. Health Part A. 2005; 68:999. [PubMed: 16020188]

[37]. Dinu CZ, Bale SS, Chrisey DB, Dordick JS. Adv. Mater. 2009; 21:1182.

[38]. Liu J, Rinzler AG, Dai HJ, Hafner JH, Bradley RK, Boul PJ, Lu A, Iverson T, Shelimov K, Huffman CB, Rodriguez-Macias F, Shon YS, Lee TR, Colbert DT, Smalley RE. Science. 1998; 280:1253. [PubMed: 9596576]

[39]. a) Marcolongo G, Ruaro G, Gobbo M, Meneghetti M. Chem. Commun. 2007:4925.b) Datsyuk V, Kalyva M, Papagelis K, Parthenios J, Tasis D, Siokou A, Kallitsis I, Galiotis C. Carbon. 2008; 46:833.

[40]. Rheinlaender J, Geisse NA, Proksch R, Schaffer TE. Langmuir. 2011; 27:697. [PubMed: 21158392]

[41]. Rotsch C, Jacobson K, Radmacher M. P Natl Acad Sci USA. 1999; 96:921.

[42]. Radmacher M, Fritz M, Kacher CM, Cleveland JP, Hansma PK. Biophys. J. 1996; 70:556. [PubMed: 8770233]

[43]. Rico F, Alcaraz J, Fredberg JJ, Navajas D. Int. J. Nanotechnol. 2005; 2:180.

[44]. Ruiz JP, Pelaez D, Dias J, Cheung HS. Cell Health Cytoskelet. 2012; 4:29. [PubMed: 23060733]

[45]. Xu WW, Mezencev R, Kim B, McDonald J, Sulchek T. Plos One. 2012; 7

[46]. Dinu CZ, Bale SS, Zhu GY, Dordick JS. Small. 2009; 5:310. [PubMed: 19148890]

[47]. a) Tusher VG, Tibshirani R, Chu G. Proc. Natl. Acad. Sci. U. S. A. 2001; 98:5116. [PubMed: 11309499] b) Suresh S. Nat. Nanotechnol. 2007; 2:748. [PubMed: 18654425]

[48]. Silkworth WT, Nardi IK, Scholl LM, Cimini D. Plos One. 2009; 4

[49]. Laurent VM, Kasas S, Yersin A, Schaffer TE, Catsicas S, Dietler G, Verkhovsky AB, Meister JJ. Biophys. J. 2005; 89:667. [PubMed: 15849253]

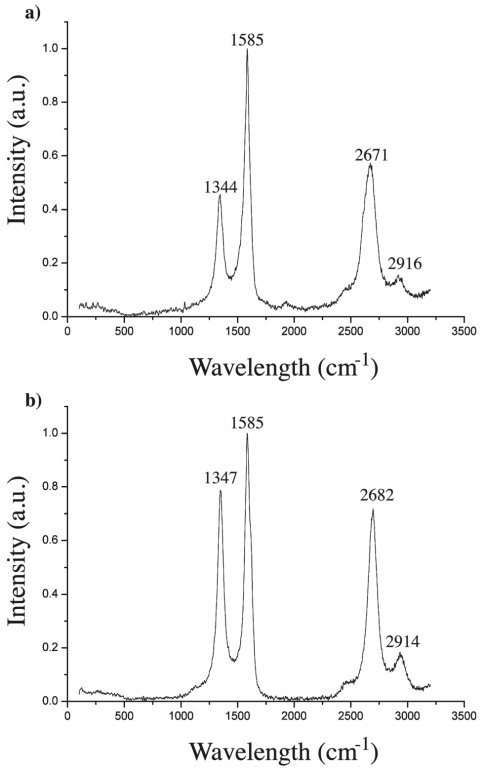


**Figure 1.**

Raman spectra of pristine and 1 h acids-washed MWCNTs. (a) Pristine MWCNTs. (b) 1 h acids-washed MWCNTs. Four independent bands have been identified for both samples, i.e., D band around 1340 $cm^{-1}$, G band at 1585 $cm^{-1}$, G' band around 2670 $cm^{-1}$, and band around 2910 $cm^{-1}$. Shifts in these bands are noticed for the 1 h acids-washed MWCNTs samples.

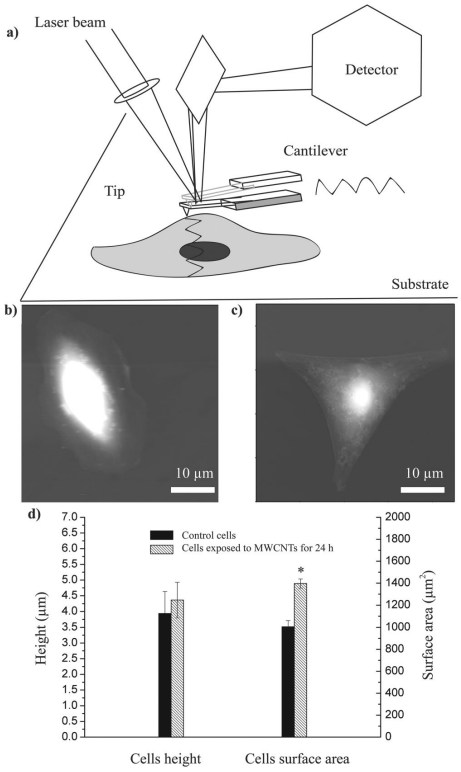


**Figure 2.**

(a) Schematic overview of the atomic force microscopy (AFM)-based analysis of epithelial cells (control and cells exposed to 1 h acids-washed MWCNTs). (b) Topography image of a control cell. (c) Topography image of a cell exposed to 1 h acids-washed MWCNTs for 24 h. The scale bar indicates 10 µm.

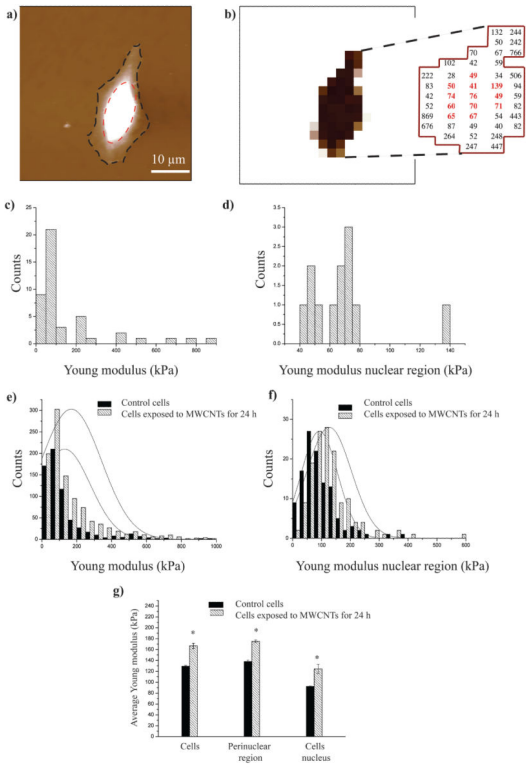


**Figure 3.**

(a) Topography image of a single control cell; the cell body is dashed black and the cell nucleus is dashed red. (b) Indentation (elastic mapping) and Young's modulus of the control cell identified in Figure 3a. (c) Histogram of the Young's modulus distribution of the single control cell shown in Figure 3a. (d) Histogram of the Young's modulus distribution of the nucleus region of the single control cell shown in Figure 3a. (e) Histogram of the Young's modulus distribution of control cells and cells exposed to 1h acids-washed MWCNTs for 24 h. The Gaussian fit reveled a considerable shift towards higher stiffness for the cells exposed to 1 h acids-washed MWCNTs. (f ) Histogram of the Young's modulus distribution of nucleus region of control cells and cells exposed to 1 h acids-washed MWCNTs for 24 h. The Gaussian fit shows that there is a considerable shift towards higher stiffness for the nucleus of the cells exposed to 1h acids-washed MWCNTs. (g) Statistical analysis of average Young's modulus distribution of control cells and cells exposed to 1 h acids-washed MWCNTs for 24 h. All differences were considered statistically significant at $p < 0.05$.

**Table 1**

Young's modulus distribution of control cells (13 individual cells were analyzed) and cells incubated with 1h acid-washed MWCNTs for 24 h (15 individual cells were analyzed). Randomized block design was used for the experimental design and data analysis.

| Group | Counts | 0–100 kPa | 100–200 kPa | 200–400 kPa | 400–600 kPa | > 600 kPa |
|---|---|---|---|---|---|---|
| Control cells | 647 | 58.89% | 25.04% | 8.96% | 5.10% | 2.31% |
| Cells incubated with 1 h acids-washed MWCNTs for 24 h | 1025 | 48.98% | 23.71% | 17.46% | 5.85% | 4.00% |
| Control cells (nucleus region) | 117 | 64.10% | 29.06% | 6.84% | 0% | 0% |
| Cells incubated with 1 h acids-washed MWCNTs for 24 h (nucleus region) | 141 | 40.43% | 48.94% | 9.23% | 1.4% | 0% |